2005-03-10

Two-Photon Ionization of the Calcium 4S3D 1D2 Level in an Optical Dipole Trap

Jared Estus Daily
Brigham Young University - Provo

TWO-PHOTON IONIZATION OF THE CALCIUM $4s3d\ ^1D_2$ LEVEL

IN AN OPTICAL DIPOLE TRAP

by

Jared Estus Daily

A thesis submitted to the faculty of

Brigham Young University

in partial fulfillment of the requirements for the degree of

Master of Science

Department of Physics and Astronomy

Brigham Young University

April 2005

BRIGHAM YOUNG UNIVERSITY

GRADUATE COMMITTEE APPROVAL

of a thesis submitted by

Jared Estus Daily

This thesis has been read by each member of the following graduate committee, and by majority vote has been found to be satisfactory.

_____   _____

Date   Scott D. Bergeson, Chair

_____   _____

Date   Dallin S. Durfee

_____   _____

Date   Mannuel Berrondo

BRIGHAM YOUNG UNIVERSITY

As chair of the candidate's graduate committee, I have read the thesis of Jared Estus Daily in its final form and have found that (1) its format, citations and bibliographical style are consistent and acceptable and fulfil university and department style requirements; (2) its illustrative materials including figures, tables and charts are in place; and (3) the final manuscript is satifactory to the graduate committee and is ready for submission to the university library.

_____   _____
Date   Scott D. Bergeson, Committee Chair

Accepted for the Department

                                 _____
                                 Ross L. Spencer, Graduate Coordinator

Accepted for the College

                                 _____
                                 Earl M. Woolley, Dean of the College of
                                 Physical and Mathematical Sciences

ABSTRACT

TWO-PHOTON IONIZATION OF THE CALCIUM $4s3d$ $^1D_2$ LEVEL

IN AN OPTICAL DIPOLE TRAP

Jared Estus Daily

Department of Physics and Astronomy

Master of Science

This thesis reports an optical dipole trap for atomic calcium. The dipole trap is loaded from a magneto-optical trap (MOT) of calcium atoms cooled near the Doppler limit (~ 1 mK). The dipole trap is formed by a large-frame argon ion laser focused to 20 μm into the center of the MOT. This laser runs single-line at 488 nm with a maximum power of 10.6 watts. These parameters result in a trap of 125 mK for calcium atoms in the $4s3d$ $^1D_2$ state.

The 488 nm light also photo-ionizes the trapped atoms due to a near-resonant transition to the $4s4f$ $^1F_3$ level. These ions leave the trap and are detected to determine the trap decay rate. By measuring this decay rate as a function of 488 nm intensity, we determine the $^1F_3$ photo-ionization cross section at this wavelength to be approximately 230 Mb.

ACKNOWLEDGMENTS

I would be quite ungrateful if I did not first thank God for my life and many blessings. I have been given much despite my many shortcomings and mistakes. I have a wonderful wife, five beautiful children, and I can ask for little more in life.

I thank my father and mother for their examples, and for all of the help and support that they have given to me and my family during our years in school. I thank my Mom for always believing me to be so much more than I am. I thank my Dad for his example as a good scientist and a good man. I also thank the rest of my family and extended family for their love, help and support.

There are many teachers and fellow students whom I could acknowledge, but I have limited space. I will give a special thanks to my advisor and friend Scott Bergeson. I thank him for his efforts and patience in teaching me the finer points of research and analysis. He has shown great care for me and for my family, and we are grateful. I thank all of the teachers and students whom I have worked with and learned from, for they are responsible for making me into a much better student and person.

I must once again thank God for my wife, Jeanne. Without her I could not have done this, and in fact I would have little reason to. She has inspired good in me more than any person I have met. She is the best mother I know, and she is the dearest friend I have. Jeanne, thank you for your patience, your kindness, your confidence, your time, your goodness, and above all, your love.

Contents

List of Figures

Chapter 1

Introduction

The field of laser-cooling and trapping of neutral atoms has seen tremendous growth over the past few decades, spurring many new developments in atomic physics. Early laser-cooling was done mostly with alkali metals due to the simplicity of their energy level structure and the availability of tunable lasers. These experiments led to the invention of the magneto-optical trap (MOT) and the optical dipole trap — two of the most widely-used tools in laser-cooling today. The use of these traps resulted directly in more precise frequency standards, the realization of Bose-Einstein condensation, and countless other ultracold atomic experiments.

In recent years, laser-cooling experiments have expanded to group II metals. This is mainly due to the general growing interest in optical frequency standards[1,2,3]. Calcium, strontium, and ytterbium all have narrow resonances from the ground state at relatively convenient laser wavelengths. By locking a laser to one of these resonances in the optical spectrum, a frequency standard with considerably improved precision over present frequency standards could be achieved. The major isotopes of these elements also have no angular momentum in the ground state, making these narrow "clock" transition frequencies less sensitive to external fields. This leads to increased

precision due to the stability in an optical frequency standard under typical laboratory conditions. Other experiments, such as ultracold plasmas, metastable collision studies, photo-associative spectroscopy, quasi-molecule formation, and Bose-Einstein condensation in simple atomic systems also contribute to the growing interest in laser-cooling alkaline-earth metals.

Despite this growing interest, only a few experiments have explored optical dipole traps for any of the alkaline-earth atoms. Dipole traps in Group I atoms are usually loaded from sub milliKelvin magneto-optical traps that utilize cooling mechanisms dependent on the angular momentum in the ground state. Without this enhanced cooling, a Group II magneto-optical trap has a relatively high temperature, which complicates the loading of optical potentials only a few milliKelvin deep[4]. However, quenched cooling techniques can reduce atomic temperatures to the microkelvin regime[5,6], and dipole traps in Sr[7,8] and Yb[9,10] have been reported. We are also aware of a ground-state calcium dipole trap reported in a Ph.D. thesis[11].

We report a new optical dipole trap in calcium. Our trap captures 2 mK atoms in the excited $4s3d\ ^1D_2$ metastable state. Due to the relatively high atomic temperature, the dipole trap operates in the regime where the light-shift is several times larger than the natural atomic transition linewidth[12]. The high intensities required to capture these relatively hot atoms are also high enough to photo-ionize them. By measuring the photo-ionization production rate and the trap lifetime as a function of dipole trap laser intensity, we determine the effective $^1D_2$ lifetime in our system and the photon-ionization cross section.

Chapter 2

Background

2.1 Radiation Pressure

In the seventeenth century, Johannes Kepler speculated that the intense light from the Sun pushes on comet tails. More than two hundred years later modern physicists confirmed his hypothesis, and began to explain how light affects matter. James Maxwell derived a value for this "radiation pressure". Max Planck discovered the quantized nature of atomic emissions. Albert Einstein suggested that light itself is quantized, and Luis deBroglie hypothesized that photons carry momentum. These fundamental discoveries all play essential roles in laser-cooling. When an atom absorbs resonant light it also absorbs the momentum in the direction of the light's propagation. The light pushes the atom, and the energy of the absorbed photon excites the atom. As the atom decays, it releases another photon in a random direction. Over many cycles the average momentum from the random emissions is zero and the photons push the atom in the direction of their initial propagation.

The earliest laboratory demonstration of radiation pressure on neutral atoms was in 1933 when Robert Otto Frisch reported the deflection of a beam of sodium atoms by resonant light from an emission lamp[13]. For the next few decades little else was

accomplished or even attempted due to the limitations in wavelength and intensity of available light sources. However, after the advent of the laser in the 1960's came the first real possibilities of studying the effects of radiation pressure on atoms. In 1970, Arthur Ashkin at Bell Laboratories accelerated and trapped microscopic dielectric spheres suspended in liquids and gases using an Ar-ion laser[14]. Ashkin also hypothesized that atoms and molecules could be accelerated and trapped using similar techniques with radiation pressure. Over the next decade, the development of tunable lasers made available the tools necessary to test his hypothesis.

2.2   Laser-cooling of neutral atoms

Most of the pioneering work in laser-cooling took place in two laboratories starting in the late seventies. Bill Phillips and Hal Metcalf led the efforts at The National Bureau of Standards (now NIST in Gaithersburg). They loaded magnetic traps by slowing and cooling atomic beams in one dimension with near-resonant lasers. An inhomogeneous magnetic field along the beam path Zeeman-shifted the atoms into resonance with the laser. The field was tapered in strength so that atoms of many temperatures or speeds could be shifted into resonance as the atomic beam cooled. This coordinate dependent cooling was the first significant demonstration of laser-cooling in neutral atoms[15,16].

At Bell Labs, Steven Chu and Arthur Ashkin studied optical potentials for neutral atoms. They were first to report 3-dimensional laser-cooling with near-resonant light in what is now called optical molasses[17], and they loaded an optical dipole trap from an optical molasses[18]. Soon after, they were the first to demonstrate the magneto-optical trap[19], which combines the 3-dimensional molasses with an inhomegeneous magnetic field superimposed on the molasses. The combined effects of the magnetic field and the optical molasses exerts a restoring force on atoms leaving the trap.

Chapter 3

Magneto-optical trap

The magneto-optical trap (MOT) is probably the most-utilized method for laser-cooling neutral atoms. The apparatus consists of three orthogonal pairs of counter-propagating laser beams for an optical molasses, a magnetic quadrapole field, and an atomic vapor source. Combining the effects of the optical molasses with the magnetic field simultaneously cools and traps a sample of thermal atoms.

The lasers forming the optical molasses are circularly polarized such that an atom at the center of the trap encounters one $\sigma+$ and one $\sigma-$ polarized beam from each direction in each dimension. The laser frequency is tuned below the atomic resonance transition. The magnetic quadrapole field is created by a pair of anti-Helmholtz coils (coils which share the same axis and carry equal but opposing currents). The coils are equidistant from the center of the optical molasses, making a magnetic field which cancels at this point and increases linearly in magnitude with radius.

In each of the three dimensions, the magnetic field shifts the energy of one of the magnetic spin sub-levels closer to resonance with the detuned MOT laser beams. The sign of the now resonant sub-level determines which type of polarization (and therefore which beam in each dimension) the atom will scatter most effectively. This
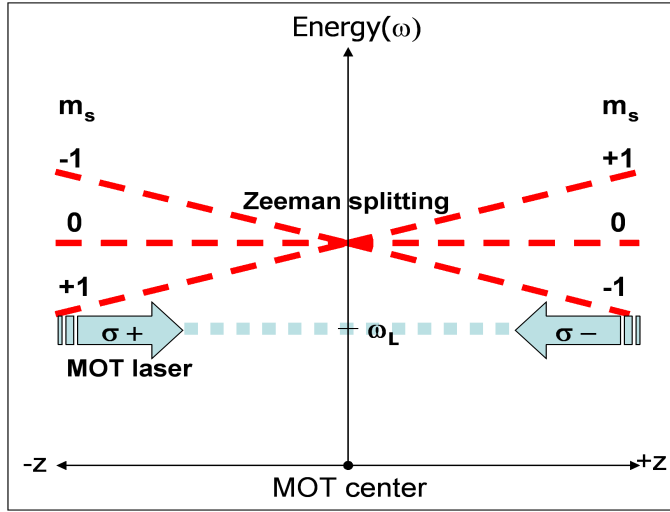
Figure 3.1: Energy diagram for atoms in a MOT. Note the increasing shift into resonance with the laser as atoms leave the MOT center.

effect results in a coordinate-dependent restoring force which constitutes the trap (See Fig. 3.1).

3.1   Lasers and optics

Our laser-cooling scheme for calcium uses the $4s^2\ ^1S_0\ \rightarrow\ 4s4p\ ^1P_1$ transition. The 423 nm light resonant with this transition is generated by frequency-doubling infrared light from a master-oscillator-power-amplifier (MOPA) system[20]. The MOPA delivers 300 mW of single-frequency light at 846 nm to a build-up cavity as shown in Fig. 3.2. This laser is phase-locked to the build-up cavity using the Pound-Drever-Hall[21] technique, giving a intensity enhancement of 30. A 10mm long a-cut $KNbO_3$ crystal in the small waist of the build-up cavity is used to generate 45 mW of output power at 423 nm via non-critical phase matching at a temperature of $-12°$ C. The laser is further stabilized by locking the 423 nm light to the calcium resonance transition using saturated absorption spectroscopy in a calcium vapor cell[22].
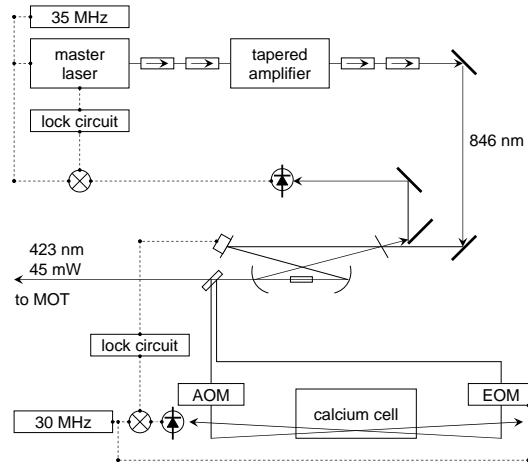
Figure 3.2: A schematic drawing of the MOT laser system and frequency stabilization electronics used in these experiments.

An acousto-optic modulator (AOM) in one arm of the saturated absorption laser beams shifts the laser frequency so that the laser beam sent to the MOT is 35 MHz (one natural line-width) below the atomic resonance. We also use this AOM to chop the laser beam and use a lock-in amplifier to eliminate the Doppler background in the saturated absorption signal. Because the 846 nm laser is already locked to the frequency-doubling cavity, the feedback from this second lock circuit servos the frequency-doubling cavity length.

3.2 Magnetic quadrapole field coils

One of my first projects was to design and build new magnetic field coils. The coils are made from insulated 1/4 inch copper refrigeration tubing, wound into two identical coils with four stacks of four concentric loops. The magnetic field is generated by 175 amps of DC current, and the coils are cooled with 10°C water. The divergence of the field is 100 Gauss/cm at the center of the MOT. The small number of coils reduces the inductance, allowing the field to be turned on and off in a few hundreds

of microseconds. This rapid turn-off is required for probing atoms in a field-free environment.

3.3   Calcium atom source

The MOT is loaded from a thermal beam of calcium atoms passing through the center of the MOT. The thermal beam is formed by heating calcium in a stainless steel oven to 650° C. The beam is weakly collimated by the 1mm diameter, 10mm long aperture in the oven wall. An additional red-detuned (140 MHz, or four times the natural line-width) laser beam counter-propagates the calcium atomic beam. This "slower beam" significantly enhances the MOT's capture efficiency. The slower beam is focused onto the oven aperture, which introduces a negative radial component into this cooling process to help maintain the collimation. As the beam passes through the MOT, the slowest atoms in the velocity distribution are cooled and trapped.

3.4   Ca MOT features

The calcium MOT in our lab traps about 6×10^6 atoms at a temperature limited by the line-width of the cooling transition. This limit is called the Doppler limit, and for this experiment it is about 1 mK. The density profile of the MOT is approximately Gaussian, with a $1/e^2$-radius of 0.5 mm and a peak density of 9×10^9 cm^{-3}. The lifetime of the MOT is limited by collisions and optical pumping to the $4s3d \ ^1D_2$ metastable state to about 10 ms.

Chapter 4

Optical dipole trap

Although difficult in practice, an optical dipole trap is simple in concept and design. The trap is formed at the focus of an off-resonant laser in a sample of atoms. The electric field of the laser induces a dipole moment in each atom. If the laser wavelength is below resonance with a particular atomic transition, the dipoles seek the region of lowest potential energy (highest electric field). Therefore, the Gaussian intensity profile of the beam and the focusing define the spatial dimensions of the trap.

4.1   Initial experiments

Our initial attempts at optical trapping were somewhat naive. We ran the Ar-ion laser at full power over all lines of the spectrum. We expected several different potentials in various states. There were two major problems with this experiment. First, we originally installed the laser on a table more than 5 meters from the MOT (where we would load the trap). Any and all instabilities at the laser were greatly amplified over the long lever-arm of the beam path. We measured the focus stability and found that it moved significantly on the time scale of the expected trap lifetimes. Any trapped atoms would be heated by this dynamic potential and ejected from the trap. The second problem was in the complex energy level structure of calcium. The

number of transitions combined with the many laser wavelengths used resulted in too many potentials and near-resonances to keep track of. The laser now sits on a 3 ft. thick, damped table adjacent to the MOT table, and all subsequent attempts at trapping were done using a single laser line.

The first few attempts at single-frequency dipole traps also failed, but this time due to difficulties in detecting the trap. We attempted one trap at 457 nm, and another at 514 nm. Both of these wavelengths create potentials of $\sim 2-6$ mK for the states in the calcium MOT. However, for ground state traps the collision rate with the background atoms is so high that atoms are ejected from the trap on the millisecond timescale — a short time compared to the time required to eliminate background atoms. In addition, the mechanism we use to detect the trap is photo-ionization. With the exception of the 488nm trap, we used an ultraviolet pulse laser to ionize the atoms. The scattered UV light on the inside of the MOT chamber created far too much background in all instances to extract any meaningful signal.

Although these early attempts at a dipole trap failed, they taught us the theoretical and practical concepts necessary to succeed. We were able to create and detect a unique dipole trap using unique methods. These first experiments were key in this process.

4.2   Optical potential

The interaction of the laser beam with the atoms is easily described in terms of the AC-Stark shift. The electric field of the laser beam $\vec{E}$ induces a polarization $\vec{P}$ in the atom, giving rise to the $-\vec{P} \cdot \vec{E}$ potential. A rotating wave approximation of this interaction leads to the well-known optical potential or "light shift"[23]:

$$U = \frac{\hbar \gamma^2}{8\Delta} \frac{I(r)}{I_s}, \tag{4.1}$$

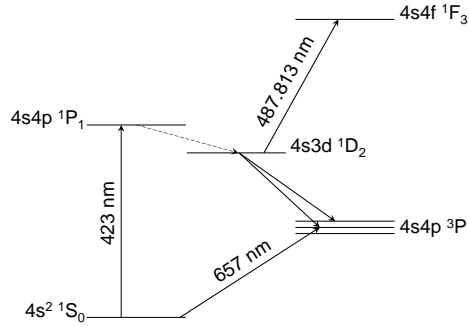where $\hbar$ is Planck's constant divided by 2π, $\gamma = \tau^{-1}$ is 2π times the natural line-

Figure 4.1: A partial energy-level diagram for calcium (not to scale).

width, and $I_s = \pi h c \gamma / 3\lambda^3$ is the saturation intensity, c is the speed of light, λ is the wavelength of the atomic transition, $\Delta = \omega - \omega_0$ is the detuning of the laser ω from the atomic transition ω_0 in rad/s, and $I(r)$ is the intensity of the laser beam. For multi-level atoms with many transitions from a given state (as in Fig. 4.1), the light shift calculation in Eq. 4.1 is extended by summing contributions from all of the transitions connected to the level, replacing γ with the appropriate line-widths.

4.3   Wavelength Selection

The detuning in Eq. 4.1 determines the sign of the optical potential, and therefore determines whether it is repulsive or attractive to the induced dipoles of the atoms. Again, for multilevel atoms, this must be considered for all states of interest. Because we load the dipole trap from the calcium MOT, the states that must be considered are all those states in the cooling cycle in Fig. 4.1. Fig. 4.2 plots the optical potential from Eq. 4.1 as a function of wavelength. The Einstein A-coefficients and natural line-widths for the calcium MOT levels come from available databases[24,25].

It is evident from Fig. 4.2(a) that the complex structure of calcium makes a dipole trap difficult to achieve. A particular wavelength may create a strong attractive potential for one state but be repulsive for another. The only practical possibility
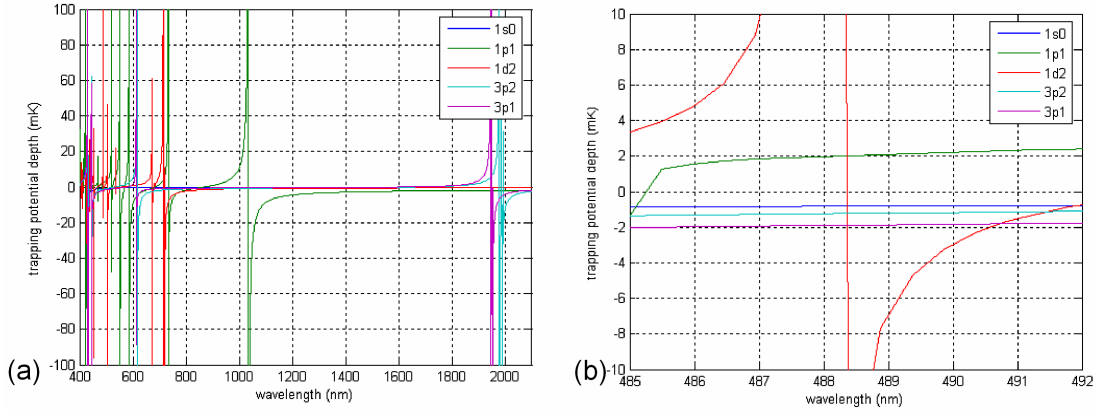
Figure 4.2: (a)Optical potential for Ca I atoms vs. wavelength. The potential for each level in the MOT cooling cycle is plotted in a separate color. Negative potentials are attractive, and positive potentials are repulsive. (b)Optical potential near 488nm.

(using relatively simple methods and available lasers) is at 488 nm, as shown in Fig. 4.2(b). We can ignore the slightly repulsive potential for the $^1P_1$ state because the atoms decay very quickly to the $^1D_2$ level.

4.4   Loading the dipole trap

The calcium dipole trap is formed by focusing a 488 nm argon-ion laser into the center of the calcium MOT. The 488 nm wavelength is near-resonant with the $4s3d \ ^1D_2 \ \rightarrow \ 4s4f \ ^1F_3$ transition ($\Delta \ = \ 2\pi c(1/487.9863\text{nm} - 1/487.8126\text{nm}) \ = -1.38 \times 10^{12}$). A 1 W laser beam focused to a 20μm Gaussian waist makes an optical potential depth of $U/k_B \ = \ 11.6$ mK. This deep potential is required to trap our relatively hot calcium atoms.

The dipole trap loads while the MOT light is on. The dipole trap fills up with atoms optically pumped into the $^1D_2$ state in the region of the 488 nm laser beam focus. Any $^1D_2$ atoms formed outside the focal region may pass through the dipole trap, but there is no dissipative cooling mechanism to capture them.
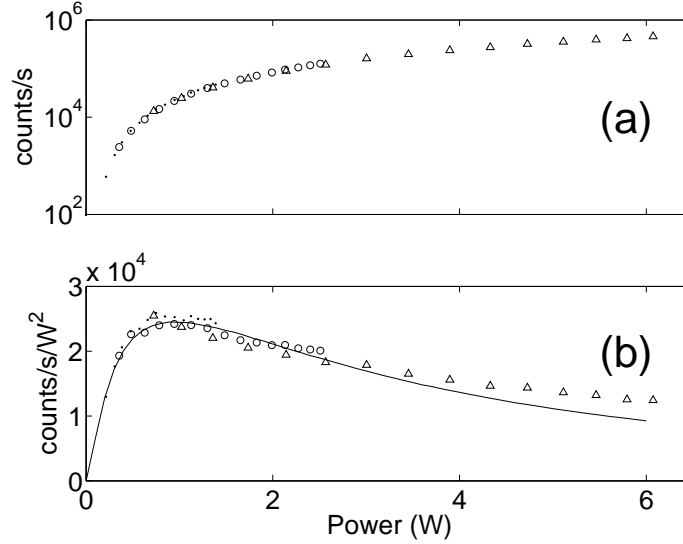
Figure 4.3: Ion count rate versus 488 nm laser power. The top panel (a) plots the raw count rate for a (measured) Gaussian waist of $w_0 = 20\ \mu$m. The laser power was changed by varying the argon-ion laser tube current. The different symbols show measurements made with different intracavity laser apertures. The lower panel (b) plots the ion count rate divided by the square of the laser power, which is proportional to the number of $^1D_2$ atoms in the dipole trap. The solid line is a fit of a Monte-Carlo simulation of trap loading to the data.

4.5   Photo-ionization and detection

Some of the trapped $^1D_2$ atoms are ionized by the 488 nm laser beam via a two-photon transition to the continuum. This photo-ionization pathway is enhanced by the near-resonance with the $^1F_3$ level, the same resonance which makes such a deep trap. As discussed below, the photo-ionization is probably further enhanced by a near-resonance in the Rydberg series leading up to the Ca II $3d$ ionization limit.

We measure the ion production rate for different 488 nm laser beam intensities [*]. Sample data is plotted in Fig. 4.3(a). This data is re-plotted in Fig. 4.3(b) with the ion production rate divided by the laser power squared. This ratio is proportional to the number of $^1D_2$ atoms in the laser focus, and in the absence of a dipole trap, this signal should be a flat line. At low powers, the number of atoms in the dipole trap increases as the trap depth increases. The trap number maximizes when the average well depth is a few times the Doppler temperature. At higher power, the trap number fall off because the 488 nm laser beam shifts the $4s^2\ ^1S_0$ and $4s4p\ ^1P_1$ levels out of resonance with the MOT laser, reducing the efficiency of the optical pumping loading mechanism. We performed a Monte-Carlo simulation of trap loading and found agreement with our data, as plotted in Fig. 4.3b.

At higher laser powers, the ion production rate is somewhat higher than expected. This occurs when the light-shift of the $^1S_0$ and $^1P_1$ levels due to the 488 nm laser beam exceeds the natural line-width. This is precisely the condition under which ground-state atoms can be captured in the dipole trap. For these atoms, the trap depth is comparable to the atom temperature (the Doppler cooling limit). Such an arrangement would increase the density of ground-state atoms, making the loading rate due to optical pumping higher at higher powers.

4.6   Trap features

We can estimate the number of $^1D_2$ atoms in our dipole trap using a simple rate equation. For deep optical potentials in steady state conditions, this is equal to the trap loading rate multiplied by the trap lifetime. The loading rate is equal to the number of ground state atoms in the trap, multiplied by the optical pumping rate, multiplied by the ratio of the trap volumes. Because the confocal parameter of the 488

---

[*]A weak electric field ($\sim$5 V/cm) applied across the MOT extracts the ions. The ions are detected using a channeltron (Burle model 4860) and counted in a multichannel scaler.

nm laser beam exceeds the MOT dimension, and because the dipole trap oscillation period along the symmetry axis is long compared to the $^1D_2$ lifetime, we can assume that the volume ratio is the square of the laser beam waist divided by the square of the Gaussian size of the MOT. The number of $^1D_2$ atoms in the dipole trap, N_D, can be written as

$$N_D = \frac{s/2}{1 + s + (2\Delta/\gamma)^2} \tau_{\text{eff}} A N_S \left(\frac{w_0^2}{2r_0^2} \right),\tag{4.2}$$

where $s = I/I_s$ is the saturation parameter for the $^1S_0 \rightarrow^1 P_1$ MOT transition, N_S is the number of ground state atoms in the trap, τ_{eff} is the dipole trap lifetime, $A = 2150$ s^{-1} is the Einstein A coefficient for the $^1P_1 \rightarrow^1 D_2$ transition, w_0 is the waist of the 488 nm beam focus, and r_0 is the Gaussian $1/e^2$ radius of the MOT. Depending on the beam waist and laser power, this simple model implies that we load up to ~ 2000 atoms into the trap, for a peak density of approximately 5×10^8 cm^{-3}. By comparison, the background density of $^1D_2$ atoms is given by Eq. 4.2 without the volume ratio, and with the numbers N_D and N_S replaced by densities. The $^1D_2$ background density is $\sim 10^7$ cm^{-3}.

It is perhaps surprising that at the lowest laser powers we can detect a small number of atoms in the dipole trap, and discriminate against the background $^1D_2$ atoms. But the background atoms roll through the trap in a few μs, while trapped atoms remain in the trap approximately 100 times longer. The photo-ionization probability increases with the time spent in the 488 nm laser focus, so the ionization signal is predominantly from the trapped atoms.

4.7 Two-photon photo-ionization rate

We measure the lifetime of the dipole trap by blocking the MOT laser beams, and measuring the decay of the ion signal. The three most important decay mechanisms are radiative decay of the $^1D_2$ level, collisional decay due to hot atoms from the

thermal atomic beam, and two-photon ionization of the $^1D_2$ atoms. Because we do not have a suitable method for turning off the thermal beam, we cannot reliably extract the $^1D_2$ radiative lifetime. Published values of the lifetime are around 2 ms [26,27,28,29,30], somewhat longer than measured in our experiment. While our experiment cannot determine the radiative lifetime, by measuring the decay rate as a function of 488 nm laser intensity we can determine the photo-ionization cross-section.

A rate-equation for $^1D_2$ level decay in the dipole trap after the loading has turned off is

$$\frac{dN_D}{dt} = -N_D \left(\frac{1}{\tau_{\text{eff}}} + \mathcal{A}I^2 \right),\tag{4.3}$$

where τ_{eff} is the lifetime of the trap extrapolated to zero power, and $\mathcal{A}$ is the two-photon ionization rate coefficient. This has the well-known solution

$$N_D(t) = N_D(0) \exp\left(\frac{1}{\tau_{\text{eff}}} + \mathcal{A}I^2 \right).\tag{4.4}$$

In second-order perturbation theory, two-photon ionization is written as an overlap of the initial and final states, divided by an energy denominator and summed over all possible intermediate states. For near-resonant ionization, the energy denominator makes the near-resonant term dominant, collapsing the sum to just one term. This one term looks like the product of the probability that an atom is excited into the $^1F_3$ state multiplied by the probability of photo-ionizing out of that state. We can write this term as

$$\mathcal{A}I^2 = \frac{s/2}{1 + s + (2\Delta/\gamma)^2}\frac{I}{h\nu}\sigma\tag{4.5}$$

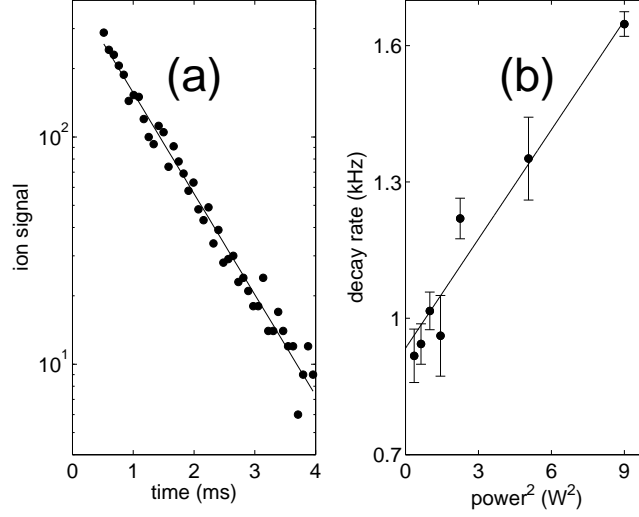$$= \frac{3\lambda^4\sigma\gamma}{8\pi h^2 c^2 \Delta^2}I^2,\tag{4.6}$$

Figure 4.4: Dipole trap decay versus power squared. The decay signal from the dipole trap. The left panel (a) shows the ion signal versus time with 1 W focused to a 90 μm waist. The effective decay rate for this data is 1.02 kHz. The right panel (b) shows the apparent decay rate for a range of powers, all focused to a 90 μm waist. The decay rate is fit to a line in square of the power, as suggested by Eq. 4.3.

where σ is the $^1F_3$ one-photon photo-ionization cross section. The approximation in Eq. 4.6 assumes that $s \ll (2\pi\Delta/\gamma)^2$ and $\gamma \ll \Delta$. In our experiment, the intensity of the 488 nm laser has a Gaussian spatial profile. Averaging the square of the intensity over the laser profile allows us to relate the photo-ionization rate to the total laser power. In this case, it can be written as

$$\mathcal{A}I^2 = \frac{\lambda^4\sigma\gamma}{2\pi^3h^2c^2\Delta^2w_0^4}P^2. \tag{4.7}$$

The dipole trap decay rate as a function of the square of the 488 nm laser power squared is shown in Fig. 4.4. For each power level, we measured the dipole trap decay. At sufficiently low power levels, this decay is approximately exponential, and

we extract the decay rate using a least-squares fitting routine [†]. The decay rate depends on power. The zero-extrapolated decay rate is $\tau_{\text{eff}}^{-1} = 0.93$ kHz. This rate is approximately twice the radiative decay rate. We see evidence in our experiment that our rate is significantly influenced by collisions with atoms in the thermal atomic beam. This is not surprising because the dipole trap sits in the middle of the thermal atomic beam. Without detailed characterization of the thermal beam, we cannot reliably extract a thermal-atom-$^1D_2$-atom collision cross-section.

4.8   Photo-ionization cross section

The slope of the decay rate with power is 80 Hz/W^2. Using Eq. 4.7, we can determine the $^1F_3$ photo-ionization cross section. This gives a photo-ionization cross-section for the $^1F_3$ level of $\sigma = 230 \times 10^{-18}$ cm^2. This extraordinarily large cross section suggests that the final state lies near a Rydberg state in the continuum. The final state is 133 cm^{-1} below the Ca II $^2D_{3/2}$ ionization limit. The principle quantum of hydrogenic Rydberg levels in this region are $n \sim 29$, and the separation between levels is 9 cm^{-1}. Our measurements are carried out in the presence of an electric field, further increasing the probability of finding a nearby Rydberg level. The NIST database tabulates only odd parity levels in this energy region. We are unaware of applicable quantum defect calculations or measurements.

[†]The trap depth is proportional to I, and the photoionization signal is proportional to I^2. At high laser powers, when atoms can be trapped even at large radii, it is possible that kinetic effects will skew the photo-ionization signal. Atoms trapped at the bottom of the potential will be ionized first, and atoms trapped at the edge of the potential will be ionized at a later time. For low enough laser powers, when the potential is too shallow to trap significant numbers of atoms, this effect should not influence the photo-ionization signal.

Chapter 5

Conclusion

We have demonstrated an optical dipole trap for neutral calcium atoms. These atoms are non-adiabatically loaded into the trap by an optical pumping mechanism. The lifetime of our trap is limited by the ~ 2 ms lifetime of the $^1D_2$ atoms and by collisions with atoms in the thermal atomic beam.

Our initial interest in the calcium optical dipole trap was its potential application to our ultracold plasma research. It may be possible to use the dipole trap as the beginning point for ultracold plasma expansion studies. Because of the high aspect ratio, a plasma generated from a dipole trap would be a two-dimensional ultracold neutral plasma at early times. Correlation heating would be reduced compared to the three-dimensional case[31], bringing the two-dimensional plasma closer to the strongly-coupled regime. Furthermore, the plasma expansion depends on the exact density distribution of the initial cloud. Compared to standard MOT traps, a dipole trap has a well-defined density profile, meaning that these new plasmas could greatly improve the reproducibility of plasma expansion experiments. We plan to explore these possibilities in future work.

Bibliography

[1] F. Ruschewitz, J. L. Peng, H. Hinderthr, N. Schaffrath, K. Sengstock, and W. Ertmer, Phys. Rev. Lett. **80**, 3173 (1998)

[2] C. W. Oates , F. Bondu, R. W. Fox , and L. Hollberg, Eur. Phys. J. D **7**, 449 (1999)

[3] F. Riehle et al., IEEE Trans. Instrum. Meas. **48**, 613 (1999)

[4] We note that sub-Doppler single-stage cooling of the odd-isotope ^{87}Sr was demonstrated in Xinye Xu, Thomas H. Loftus, Josh W. Dunn, Chris H. Greene, John L. Hall, Alan Gallagher, and Jun Ye, Phys. Rev. Lett. **90**, 193002 (2003)

[5] E. A. Curtis, C. W. Oates, and L. Hollberg, J. Opt. Soc. Am. B **20** 977 (2003)

[6] T. Binnewies et al., Phys. Rev. Lett. 87, 123002 (2001)

[7] H. Katori, T. Ido, and M. K.-Gonokami, J. Phys. Soc. Japan **68**, 2479 (1999)

[8] M. Takamoto and H. Katori, Phys. Rev. Lett. **91**, 223001 (2003)

[9] Y. Takasu et al, Phys. Rev. Lett. 90, 023003 (2003)

[10] Y. Takasu et al., Phys. Rev. Lett. 91, 040404 (2003)

[11] Carsten Degenhardt, "Free and trapped calcium atoms for an optical frequency standard," Ph.D. thesis, University of Hannover (2004). Chapter 5 in this thesis describes a dipole trap created with an Ar-ion laser at 514 nm. They focused 8 W to a waist of 150 μm for a trap depth of roughly 30 μK. They loaded the dipole trap from an ultracold ensemble of "quench-cooled" atoms.

[12] J. D. Miller, R. A. Cline, and D. J. Heinzen, Phys. Rev. A **47**, R4567 (1993)

[13] R. Frisch, Zeit. für Phys. **86**, 42 (1933)

[14] A. Ashkin, Phys. Rev. Lett. **24**, 156 (1970)

[15] J. V. Prodan, W. D. Phillips, and H. Metcalf, Phys. Rev. Lett. **49**, 1149 (1982)

[16] W. Phillips and H. Metcalf, Phys. Rev. Lett. **48**, 596 (1982)

[17] S. Chu, J. L. Peng, H. Hinderthr, N. Schaffrath, K. Sengstock, and W. Ertmer, Phys. Rev. Lett. **55**, 48 (1985)

[18] S. Chu, J. E. Bjorkholm, A. Ashkin, and A. Cable, Phys. Rev. Lett., **57**, 314 (1986)

[19] E. L. Raab, M. Prentiss, Alex Cable, Steven Chu, and D. E. Pritchard Phys. Rev. Lett. 59, 2631 (1987)

[20] A. D. Ludlow, H. M. Nelson, and S. D. Bergeson J. Opt. Soc. Am. B **18**, 1813 (2001)

[21] R. W. P. Drever, J. L. Hall, F. V. Kowalski, J. Hough, G. M. Ford, A. J. Munley, and H. Ward, Appl. Phys. B **31** 97 (1983)

[22] K. G. Libbrecht, R. A. Boyd, P. A. Willems, T. L. Gustavson, and D. K. Kim Am. J. Phys. **63**, 729 (1995)

[23] Harold J. Metcalf and Peter Van Der Straten, *Laser Cooling and Trapping* (Springer-Verlag, New York, NY 1999)

[24] The NIST Atomic Data Center critically evaluates and compiles transition probability data. It can be accessed through their web site at http://physics.nist.gov/cgi-bin/AtData/main_asd . The paper version of the data for calcium can be found in *Atomic Transition Probabilities (Na through Ca - A Critical Data Compilation)*, W. L. Wiese, M. W. Smith, and B. M. Miles, Natl Stand. Ref. Data Ser., Natl Bur. Stand. (U.S.), NSRDS-NBS 22, Vol. II (1969). Improved transition probabilities, when available, are found in J. R. Fuhr and W. L. Wiese, "Atomic Transition Probabilities," published in *the CRC Handbook of Chemistry and Physics*, 79th Edition, edited by D. R. Lide (CRC Press, Inc., Boca Raton, FL, 1998).

[25] R.L. Kurucz and B. Bell, "1995 Atomic Line Data," Kurucz CD-ROM No. 23. Cambridge, Mass.: Smithsonian Astrophysical Observatory. This information is also available online at http://cfa-www.harvard.edu/amdata/ampdata/-kurucz23/sekur.html

[26] L. Pasternack, D. M. Silver, D. R. Yarkony, and P. J. Dagdigian, J. Phys. B **13**, 2231 (1980)

[27] D. Husain and G. Roberts, J. Chem. Soc., Faraday Trans. **2**, 1921-1933 (1986)

[28] R. Drozdowski, J. Kwela, and M. Walkiewicz, Z. Phys. D. **27**, 321 (1993)

[29] S. G. Porsev, M. G. Kozlov, Yu. G. Rakhlina, and A. Derevianko, Phys. Rev. A **64**, 012508 (2001)

[30] C. F. Fischer and G. Tachiev, Phys. Rev. A **68**, 012507 (2003)

[31] Y. C. Chen, C. E. Simien, S. Laha, P. Gupta, Y. N. Martinez, P. G. Mickelson, S. B. Nagel, and T. C. Killian, Phys. Rev. Lett. **93**, 265003 (2004)

[32] J. E. Daily, R. Gommers, E.A. Cummings, D. S. Durfee, S.D. Bergeson, Phys. Rev. A, in print (2005)

[33] C. Degenhardt, H. Stoehr, U. Sterr, F. Riehle, and C. Lisdat, Phys. Rev. A **70**, 023414 (2004)

[34] R. L. C. Filho et al., J. Opt. Soc. Am. B **20** 994 (2003)

[35] S. J. M. Kuppens, K. L. Corwin, K. W. Miller, T. E. Chupp, and C. E. Wieman, Phys. Rev. A **62** 013406 (2000)

[36] W. D. Phillips, Rev. Mod. Phys. **70** 721 (1998)

[37] J. Prodan, A. Migdall, and W. D. Phillips, Phys. Rev. Lett. **54** 992 (1985)

[38] M. Takamoto and H. Katori, Phys. Rev. Lett. **91**, 223001 (2003)

[39] B.H. Bransden and C.J. Joachain, *Physics of Atom and Molecules* (Prentice Hall, Inc., Harlow, UK 2003)

[40] Prof. Dr. Sigfried Flüge, *Practical Quantum Mechanics*, (Springer-Verlag, New York, NY 1974)

[41] David J. Griffiths, *Introduction to Quantum Mechanics*, (Prentice Hall, Inc., Upper Saddle River, NJ 1995)

[42] Eugen Merzbacher, *Quantum Mechanics* (John Wiley and Sons, Inc., New York, NY 1998)

[43] Peter W. Milonni and Joseph H. Eberly, *Lasers* (John Wiley and Sons, New York, NY 1998)

[44] Masataka Mizushima, *Quantum Mechanics of Atomic Spectra and Atomic Structure* (W.A. Benjamin, Inc., New York, NY 1970)

[45] G.K. Woodgate, *Elementary Atomic Structure*, (Oxford University Press, New York, NY 1998)